

## PAPER

Cite this: *Soft Matter*, 2014, 10, 8475

# The ratio of the lateral correlation length and particle radius determines the density profile of spherical molecules near a fluctuating membrane

 Fidel Córdoba-Valdés,<sup>abc</sup> Ramón Castañeda-Priego,<sup>\*b</sup> Jens Timmer<sup>ef</sup>  
and Christian Fleck<sup>\*cd</sup>

Interactions between membranes and molecules are important for many biological processes, e.g., transport of molecules across cell membranes. However, the detailed physical description of the membrane–biomolecule system remains a challenge and simplified schemes allow capturing its main intrinsic features. In this work, by means of Monte Carlo computer simulations, we systematically study the distribution of uncharged spherical molecules in contact with a flexible surface. Our results show that the distribution for finite size particles has the same simple functional form as the one obtained for point-like particles and depends only on the ratio of the lateral correlation length of the membrane and the radius of the molecules.

 Received 15th July 2014  
Accepted 25th August 2014

DOI: 10.1039/c4sm01550a

www.rsc.org/softmatter

## 1 Introduction

The diversity of life has been made possible by the invention of the plasma membrane which separates the interior of a cell from the environment. This outer confining envelope of cells enables cells to build up a constant inner milieu and allows selective material exchange between the cell and its environment.<sup>1</sup> A simple bacterium has only the plasma membrane, but the interior of eukaryotic cells is also structured by membranes, which enclose different intracellular compartments.<sup>2</sup> The separation into inner and outer space by membranes opened the possibility of energy storage in the form of electrochemical potential gradients, which is essential to many biological processes, e.g., the active uptake of nutrients in animal cells and signaling in neurons.<sup>3</sup> Membranes take part in enzyme activity, e.g., the bio-synthesis of phospholipids or oxidative phosphorylation and control the flow of information between cells either by recognizing signal molecules received from others cells, or by sending chemical or electrical signals to other cells.<sup>4</sup> Therefore,

membranes play an active part in the life of the cell. Biomembranes typically consist of a double layer of lipids into which different proteins are embedded.<sup>5</sup> These bilayers are generally just a few nanometers thick, with a surface area that extends over several square centimeters. In many practical situations, a sufficient description of the membrane is used to model it as a simple sheet characterized only by its elastic properties, *i.e.*, bending rigidity and surface tension.<sup>6</sup>

Many biological processes are controlled by the interactions of molecules with cell membranes. Besides highly specific interactions of steric, electrostatic and chemical nature,<sup>7,8</sup> entropic force fields are omnipresent and depend only on geometrical features. These so-called depletion forces arise because both the membrane and the molecules generate excluded volumes for the small particles forming the solvent. Although these forces have been discussed for biological systems for many years,<sup>9</sup> the simultaneous presence of many other forces severely impedes the precise analysis of depletion forces in such systems.

In recent years, there has been significant progress in understanding the depletion forces between two big spheres and between a single big sphere and a flat wall based on experiments, simulations and theoretical results.<sup>10–12</sup> In many cases, membranes are, however, not flat, but rather have surfaces of varying curvature. This leads to a modification of the depletion forces as they are no longer directed only normal to the surface, like at a flat wall or at a wall with constant curvature; there exists a lateral component of the force which promotes transport along the membrane. Recently, it has been shown experimentally that these forces are responsible, for instance, for adhesion of red blood cells to cells or surfaces.<sup>13</sup> However, to our best knowledge, there are no systematic

<sup>a</sup>UPIIG-IPN, Mineral de Valenciana 200, 36275 Silao de la Victoria, Guanajuato, Mexico

<sup>b</sup>División de Ciencias e Ingenierías, Campus León, Universidad de Guanajuato, Loma del Bosque 103, Lomas del Campestre, 37150 León, Guanajuato, Mexico. E-mail: ramoncp@fisica.ugto.mx

<sup>c</sup>Center for Biological Systems Analysis (ZBSA), University of Freiburg, Habsburgerstr. 49, 79104 Freiburg, Germany

<sup>d</sup>Laboratory for Systems and Synthetic Biology, Wageningen University, Dreijenplein 10, 6703 HB, Wageningen, The Netherlands

<sup>e</sup>Institute for Physics, University of Freiburg, Hermann-Herder-Str. 3, 79104 Freiburg, Germany

<sup>f</sup>BIOSS Centre for Biological Signaling Studies, Schänzlestr. 18, 79104 Freiburg, Germany

theoretical and simulation studies available which accurately predict the important curvature dependence of the membranes on both the depletion forces and the local microstructure of molecules in contact with the fluctuating membrane. A few theoretical cases reported by Bickel and coworkers<sup>14</sup> illustrate the importance of such effects. Nonetheless, a full description requires advanced techniques which must be adapted to study depletion potentials close to arbitrarily shaped substrates.

Molecular dynamics methods are powerful tools which could be used for studying biological membranes taking into account explicitly its molecular composition, *e.g.*, see ref. 15 and references therein. However, as these are computationally very costly for systems involving different length and time scales, *i.e.*, a suspension made up of particles with different sizes in contact with a fluctuating membrane, continuum models provide the only feasible simulation schemes.<sup>15</sup> By coarse-graining over the lipid degrees of freedom, fluid membranes have been successfully described by infinitely thin, continuous sheets with curvature elastic energy. The solvent contribution is implicitly present in the elastic properties that specify the model.<sup>16</sup> In particular, the Helfrich model has been most widely applied to the study of bilayers with small thermal height fluctuations away from a flat reference configuration.<sup>16</sup> Using this approach, we have developed a simple lattice simulation model that incorporates both the elastic degrees of freedom of the membrane and those of a suspension of biomolecules interacting with a hard-sphere potential; the explicit details of the model can be found in ref. 17 and are briefly described below.

It is important to point out that membranes are soft materials that in contrast to traditional nanostructures exhibit high susceptibility to the thermal fluctuations of the environment. Hence, as we mentioned above, this property gives rise to intriguing forces of pure entropic origin between the membrane and nanomaterials, such as polymers and colloids. A recent review on the forces that rule the interactions between membranes and molecules has been introduced by Bickel and Marques.<sup>18</sup> Furthermore, it is known that when some molecules are bounded to the membrane they deform its shape leading to important membrane-mediated interactions between molecules.<sup>19–21</sup>

Thus, the aim of this work is to understand the role of the particle–membrane interaction on the static microstructure of colloidal particles near a fluctuating membrane. We focus on the simplest model system consisting of a monodisperse suspension of hard spherical particles of finite size. We consider highly dilute suspensions to avoid the inclusion of particle–particle correlations. In particular, the particle density profile perpendicular to the membrane surface is measured for different values of the parameter space, namely, the mean roughness, lateral correlation length and particle size, in order to identify the mechanisms that determine the distribution of biomolecules in contact with the membrane; the striking finding is that the ratio between the lateral correlation and the particle size is the only relevant parameter.

After the present Introduction, Section 2 describes both the Helfrich model and our lattice simulation scheme. We also discuss the case in which the molecules behave as an ideal gas. We refer to this case as the point-like limit. In Section 3, we

present and discuss our results with particles of finite size. We mainly emphasise the entropy-driven mechanisms that lead to the shifting and tilting of the density profile. Finally, the manuscript ends with a section of concluding remarks.

## 2 Helfrich model, lattice simulation model and density profile in the point-like limit

Biological membranes are complex objects consisting of a lipid bilayer with enclosed trans-membrane proteins and attached extracellularly to the glycocalyx and intracellularly to the cytoskeleton. However, in order to understand certain aspects of the behavior of cell membranes, it is advantageous to study simpler objects composed solely of lipids. Two systems composed of a pure phospholipid bilayer are vesicles and planar bilayers. Vesicles are bags up to 100  $\mu\text{m}$  in diameter consisting of a phospholipid bilayer that encloses a central aqueous compartment.<sup>22,23</sup> They are formed by mechanically dispersing phospholipids in water. Planar bilayers are formed across a hole in a partition that separates two aqueous solutions.<sup>22,23</sup> Below, we shall confine ourselves to the discussion of the properties of membranes composed of lipids and neglect the further complexity of cell membranes.

Lipid bilayers combine exceptional elastic properties which would be difficult to obtain with synthetic materials. The bending modulus is smaller than that of a 5 nm thick shell made of polyethylene, by a factor of 1000, and the shear modulus by a factor of 10 000, but the area compression modulus is almost as large as those of the polyethylene shell, which makes the bilayer virtually incompressible.<sup>22</sup> The bending rigidity of lipid bilayers is between 5 and 100  $k_{\text{B}}T$ , with  $k_{\text{B}}$  being the Boltzmann constant and  $T$  being the absolute temperature. Due to the low bending rigidity, membranes undergo thermal shape fluctuations, which can be visualized by interference contrast microscopy.<sup>24</sup>

Keeping in mind the properties mentioned above, Helfrich proposed a Hamiltonian that describes a fluctuating membrane;<sup>16</sup> this model is discussed below.

### 2.1 Helfrich model

The Helfrich model contains only two parameters that can experimentally be measured, *i.e.*, the bending rigidity and surface tension.<sup>16</sup> This simple model considers the membrane, basically, as an elastic sheet and has been used and verified in numerous studies. For example, in experiments analyzing the fluctuation spectrum of red blood cells,<sup>25</sup> in the theoretical investigations of the steric repulsive interactions between proximal membranes,<sup>26</sup> and in studies on stacks of lipid bilayers.<sup>27</sup> Helfrich-like models with additional harmonic interactions can also be handled analytically. Equilibrium properties can be calculated for various forms of harmonic potentials, including localized pinning and uniform confinement.<sup>28–30</sup>

Within the Helfrich approximation, effects due to finite thicknesses are completely neglected. Mathematically, such a model can be described (in the limit of small fluctuations) as

follows. By using the position vector  $\mathbf{S} = \mathbf{S}(\vec{\rho}, h(\vec{\rho}))$ , where  $\vec{\rho} \in \mathcal{A}$  is the vector on the  $xy$ -plane and  $h$  is the field in the  $z$ -direction representing the membrane thermal fluctuations, the elastic membrane energy reads as<sup>6</sup>

$$H_m[h] = \frac{1}{2} \int [\kappa(\nabla^2 h)^2 + \gamma(\nabla h)^2 + \mu h^2] dx dy, \quad (1)$$

where  $\kappa$ ,  $\gamma$  and  $\mu$  are the mean bending rigidity, the surface tension and the strength of a harmonic potential, respectively.

The height–height correlation function  $G(\vec{\rho} - \vec{\rho}') = \langle h(\vec{\rho})h(\vec{\rho}') \rangle_0 - \langle h(\vec{\rho}) \rangle_0 \langle h(\vec{\rho}') \rangle_0$  permits us to evaluate the main length scales of the membrane associated with its inherent elastic properties, where the ensemble averages are calculated according to  $\langle \dots \rangle_0 = \int Dh \dots e^{-\beta H_m[h]} / \int Dh e^{-\beta H_m[h]}$ . For a membrane with vanishing surface tension, *i.e.*,  $\gamma = 0$ , the correlation function takes the following simple analytic form  $G(\vec{\rho}) = -\frac{4}{\pi} (\xi_{\perp}^0)^2 kei\left(\sqrt{2} \frac{\rho}{\xi_{\parallel}^0}\right)$ , where  $kei(x) = Im[K_0(xe^{i\pi/4})]$  is a Kelvin function,  $\xi_{\perp}^0 \equiv G(0)^{1/2} = 2^{-3/2}(\kappa\mu)^{-1/4}$  is the mean roughness of the membrane and  $\xi_{\parallel}^0 = 2^{1/2}(\kappa/\mu)^{1/4}$  is the in-plane correlation length, which is associated with the exponential decay of  $G(\mathbf{r})$  at long distances.<sup>31</sup> To understand both length scales of the membrane, we can study their limiting cases: when  $\kappa \rightarrow 0$  (where thermal fluctuations easily modify the shape of the membrane) at fixed  $\mu$  also  $\xi_{\parallel}^0 \rightarrow 0$ , but if  $\kappa \rightarrow \infty$  (flat wall) then  $\xi_{\parallel}^0 \rightarrow \infty$ , and  $\xi_{\perp}^0$  behaves inversely at both limits. In contrast, at fixed  $\kappa$  the behavior is very similar in both correlation lengths, *i.e.*, they decay  $\sim \mu^{-1/4}$  for  $\mu \rightarrow \infty$ .

Additionally, eqn (1) allows us to compute the height distribution of the membrane. It takes the following analytical form:

$$f(z) = \langle \delta(z - h(\vec{\rho})) \rangle_0 = \frac{1}{\sqrt{2\pi}\xi_{\perp}^0} \exp\left(-\frac{z^2}{2\xi_{\perp}^0{}^2}\right), \quad (2)$$

which means that the height distribution of the membrane is Gaussian, as a consequence of the fact that eqn (1) is an approximation up to the second order on the  $h$ -field.

## 2.2 Lattice simulation model

The membrane is represented as a two-dimensional  $N_L \times N_L$  square lattice with lattice constant  $a$ . The projected area of the membrane is  $A = a^2 N_L^2$ . In order to calculate the internal energy of the membrane, we use the discrete version of eqn (1). Monte Carlo simulations have been implemented according to the algorithm described in ref. 17. This algorithm has also been applied to study the aggregation behavior of two separate confined polymer chains induced by membranes.<sup>32</sup>

We have tested our simulations by calculating, for different elastic parameters, the distribution of the membrane and compared with eqn (2). The definition of  $\xi_{\perp}^0$  and  $\xi_{\parallel}^0$  is assumed to be true in the continuum limit ( $a \rightarrow 0$  and  $N_L \rightarrow \infty$ ) of an infinite membrane. In our simulations, however, we use a discrete representation. Therefore, we recall the discrete membrane roughness.<sup>33</sup>

$$\xi_{\perp}^d = \sqrt{\left(\frac{1}{N_L a}\right)^2 \sum_{n,m} K_{nm}}, \quad (3)$$

where  $K_{nm}$  is the discrete propagator of the form

$$K_{nm} = \frac{1}{\kappa f_{nm}^2 + \gamma f_{nm} + \mu}. \quad (4)$$

We have defined the matrix  $f_{nm}$  as

$$f_{nm} = \frac{2}{a^2} \left[ \cos\left(2\pi \frac{n}{N_L}\right) + \cos\left(2\pi \frac{m}{N_L}\right) - 2 \right]. \quad (5)$$

The results obtained from simulations have to be compared with these discrete quantities in order to estimate the statistical uncertainties. As long as the number of Monte Carlo steps increases, the simulated roughness,  $\xi_{\perp}^s$ , has to converge to  $\xi_{\perp}^d$  instead of  $\xi_{\perp}^0$ . In the limit  $N_L \rightarrow \infty$  and  $a \rightarrow 0$ ,  $\xi_{\perp}^d$  converges exactly to  $\xi_{\perp}^0$ . In Fig. 1, the membrane height distribution is shown and compared with the continuum limit (2). By fitting function (2), the simulated roughness  $\xi_{\perp}^s$  can be estimated. The relative difference respect to  $\xi_{\perp}^0$  is around 2%, which is the same difference as between  $\xi_{\perp}^0$  and  $\xi_{\perp}^d$ . By increasing the number of lattices and making  $a$  smaller this difference decreases below the 2%, as expected. In order to produce results in a reasonable time, we have performed simulations with the number of lattices ranging from  $80 \times 80$  to  $200 \times 200$ . In all simulations, the length of the membrane,  $L = aN_L$ , was fixed at 40.

## 2.3 Point-like limit

We consider  $N$  colloidal spherical particles of radius  $a_c$  in contact with the membrane. Their positions are characterized by the vectors  $\vec{r}_i$ ,  $i = 1, \dots, N$ . Particles interact with each other through the hard-core potential mathematically described by the relationship,

$$\beta u_{cc}(r_{ij}) = \begin{cases} \infty & r_{ij} < 2a_c \\ 0 & r_{ij} \geq 2a_c, \end{cases} \quad (6)$$

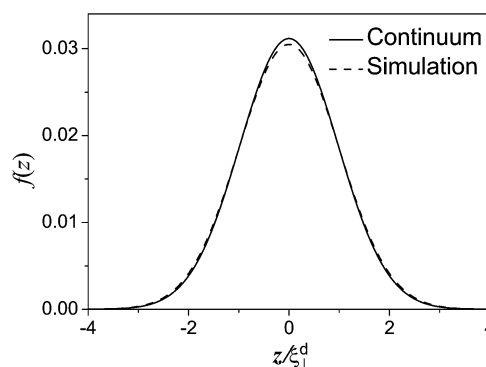


Fig. 1 Membrane height distribution. The solid line denotes the continuum limit with  $\xi_{\perp}^0 = 12.80$ . The dashed line denotes the distribution obtained by simulating an  $80 \times 80$  lattice with lattice constant  $a = 0.5$ . Then,  $\xi_{\perp}^s = 13.083$  was obtained by using eqn (2).

where  $r_{ij}$  denotes the distance between colloids. A particle located at  $\vec{r}_i = (\vec{\rho}_i, z_i)$  interacts with a membrane site located at  $\vec{R} = (\vec{\rho}, h(\vec{\rho}))$ , *i.e.*,

$$\beta u_{mc}(R_i) = \begin{cases} \infty & R_i < 0 \\ 0 & R_i \geq 0, \end{cases} \quad (7)$$

where  $R_i = \sqrt{(\vec{\rho} - \vec{\rho}_i)^2 + (h(\vec{\rho}) - z_i)^2} - a_c$  is the shortest distance from the surface of particle  $i$  to the membrane site. The partition function of the full membrane–colloid system can be written as

$$Z = \frac{1}{N!} \int \prod_i^N \frac{d\vec{r}_i}{\lambda^3} \int Dhe^{-\beta H_m(h) - \beta \sum_{j>i}^N u_{cc}(r_{ij})}, \quad (8)$$

$\lambda$  is the thermal wavelength, which results from the integration over the particle momenta.

In general, the analytical integration of the partition function is a hard task which has been simplified in a few cases. In particular, in the case of point-like particles ( $a_c = 0$ ), the partition function (8) has been calculated analytically by Bickel.<sup>34</sup> The density profile of the particles can be straightforwardly evaluated,

$$\rho(z) = \frac{1}{2} \rho_\infty \left[ 1 + \operatorname{erf} \left( \frac{z + z_0}{\sqrt{2} \xi_\perp^0} \right) \right], \quad (9)$$

where  $\rho_\infty$  is the density at the bulk and  $z_0 = \rho_\infty \mu^{-1}$  is a characteristic shift. The physical meaning of this shift can be explained as follows. When in contact with the colloidal solution, the membrane experiences the osmotic pressure of the particles and the membrane moves to a new equilibrium position given by  $z_0$ . Therefore, eqn (9) provides an excellent benchmark to test more elaborated theoretical frameworks and, of course, simulation models.

To test our lattice simulation model described above, we have carried out simulations with a  $80 \times 80$  membrane with a lattice constant  $a = 0.5$  and 400 point-like particles. For each Monte Carlo (MC) step, a trial move for all membrane patches, *i.e.*, lattice sites, and particles is accomplished.  $10^6$  Monte Carlo steps were performed to equilibrate the system, afterwards  $10^7$  MC steps were considered to calculate averages; this simulation protocol allowed us to reduce the associated uncertainties in such a way that they are smaller than the symbol size used in the plots. We compare the simulated density profile with eqn (9). In Fig. 2, density profiles for different reduced bulk densities ( $\rho_\infty^* \equiv \rho_\infty (\xi_\perp^0)^3$ ) are shown. A good agreement between simulation and theory is clearly observed. The inset shows profiles shifted by  $z_0$ ; all lying on a master curve. Shifted profiles are symmetric around the mean location of the membrane, meaning that particles are homogeneously distributed, on average, in the holes and valleys of the membrane.

### 3 Spherical finite size particles

We have seen that in the limit of vanishing particle size ( $a_c \rightarrow 0$ ), the particle profile becomes symmetric and can analytically be represented by eqn (9). Nonetheless, this limit does not take fully into account the contribution of the particle–membrane

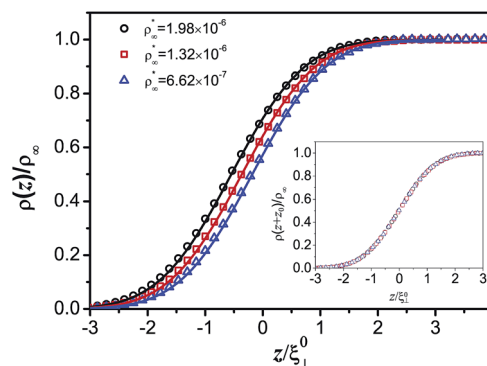


Fig. 2 Density profile of point-like particles for different reduced bulk densities,  $\rho_\infty^* \equiv \rho_\infty (\xi_\perp^0)^3$ . Solid lines show eqn (9) and symbols denote the simulation data. The inset shows the same density profiles shifted by  $z_0 = \rho_\infty / \mu$ .

interaction,  $\beta u_{mc}(R)$ , *i.e.*, particle finite size effects. However, when  $\beta u_{cm}(R)$  is taken into account explicitly one expects a completely different structural scenario that, to our best knowledge, has not been explored previously. For example, one immediately can think that the particle distribution near the membrane should change dramatically due to the interplay between different length scales, leading to new features in the particle ordering. Also, in a naive picture, one may expect morphology changes in the membrane. Then, to characterize the ordering of molecules close to fluctuating membranes, we here extend the previous results for particles with finite size. We have focused on two main contributions, namely, the membrane contribution and the particle–membrane contribution, neglecting completely correlations between particles, *i.e.*,  $\beta u_{cc}(r) \approx 0$ . This limit is reached by considering systems with very low densities ( $\rho_\infty^* \sim 10^{-5}$  or, equivalently, with a volume fraction  $\phi \sim 10^{-4}$ ).

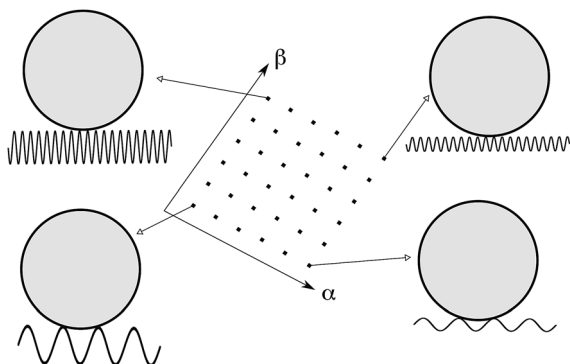
The system is now determined by three parameters that define a parameter space given by a point of the form:  $(\xi_\perp^0, \xi_\parallel^0, a_c)$ . In order to explore the parameter space, we have redefined a reduced space characterised by only two dimensionless variables:

$$\alpha \equiv 2a \mathcal{J} \xi_\perp^0, \quad (10)$$

$$\beta \equiv 2a \mathcal{J} \xi_\parallel^0. \quad (11)$$

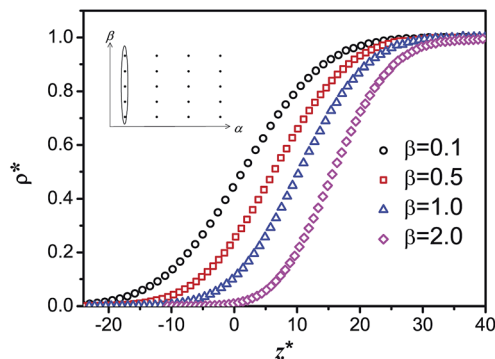
Additionally, to avoid discretisation effects in all simulations, the condition  $\xi_\parallel \gg a$  is required ( $\xi_\parallel/a \geq 4$  holds for all our simulations).

Fig. 3 shows a schematic representation of the parameter space and gives some insight into different typical configurations. In the limiting cases:  $\beta \rightarrow \infty$ , an infinity number of patches of the membrane touch the particle surface and when  $\beta \rightarrow 0$ , the contact area between the surface and the particle is reduced to one single point. A noteworthy feature of this space is that  $\beta$  is the only important parameter, since  $\alpha$  can be removed by rescaling all lengths with the roughness of the membrane as it will be shown further below.



**Fig. 3** Schematic representation of different configurations on the  $\alpha - \beta$  space. By fixing  $\beta$  and moving on  $\alpha$ , the number of points of the membrane touching the particle remains constant. On the other hand, by increasing  $\beta$ , the number of points in contact with the particle becomes larger. In this cartoon, the properties of the membrane are varied, but it is also possible to achieve similar configurations by changing the molecule size.

We have simulated different systems in the  $\alpha - \beta$  space, either by varying the membrane properties or particle sizes. Fig. 4 shows four density profiles by fixing  $\alpha$  and varying  $\beta$ . We immediately observe that the profiles are still symmetric and are also shifted in a similar manner as in the point-like case. However, as can be seen in eqn (9), the mean surface location is shifted by  $z_0$ , which is a monotonic function of the bulk density. Unfortunately, from the simulation point of view, it is difficult to have a fixed density when one deals with particles of finite size because the mean surface location is not a monotonic function of the density anymore. Nonetheless, in our simulations we have calculated the new  $z_0$  by measuring the average location of all membrane patches. In order to sort out the difficulties of changes in the particle density, we have translated all profiles to the right, by subtracting the particle radius,  $a_c$ , and  $z_0$ . Unlike the point-like case, particle profiles are shifted to the right of  $z = 0$ , and tilted as long as  $\beta$  increases. If the size of the particles becomes larger it is more unlikely that particles



**Fig. 4** Density profiles for different values of  $\beta$ . By increasing  $\beta$ , profiles show the same trend: shifting respect to  $z = 0$  and tilting.  $z$ -Axis is rescaled according to  $z^* = (z - a_c - z_0)/a_c$  and density profiles are rescaled by  $\rho^* = \rho(z)/\rho_\infty$ . On the top left, a schematic representation of the parameter space is drawn.

can access, on average, into the valleys of the membrane. This excluded volume is reflected as a shift on the distribution of particles close to the fluctuating surface.

An interesting question is whether the elastic properties of a fluctuating membrane change when it interacts with the molecules. This topic has been addressed by several authors. For example, one of us estimated a variation of the mean roughness when electrostatic interactions between point-like particles and a fluctuating membrane are explicitly considered.<sup>33</sup> Additionally, in ref. 14 and 35 changes of the membrane properties are calculated when it interacts with particles of finite size. In our case, to estimate (possible) changes on the membrane elastic properties, we have extracted the simulated roughness  $\xi_\perp^s$  by fitting the membrane height distribution obtained by means of computer simulations to the analytical height distribution function<sup>(2)</sup>. Afterwards, simulations without particles and the same initial conditions for the membrane have been carried out. By comparing both roughnesses, relative differences less than 3.2% in all our simulations were found. This means that for low particle concentrations changes of the membrane properties are absent. However, one can expect appreciable changes in systems with either higher densities or intrinsic polydispersities.

### 3.1 Shifting and tilting

In order to estimate the shifting and tilting already discussed in Fig. 4, we have fitted the density profiles using the functional form of eqn (9),

$$\rho(z) = \frac{1}{2}\rho_\infty \left[ 1 + \operatorname{erf} \left( \frac{z - p_1}{\sqrt{2}p_2} \right) \right], \quad (12)$$

where we have introduced two fitting parameters  $p_1$  and  $p_2$ . The meaning of these parameters is similar to the point-like case:  $p_1$  is the membrane shift due to the balance between the harmonic potential and the suspension pressure and  $p_2$  is an effective roughness, which can be understood as follows. For  $\beta > 1$  the particles cannot penetrate into the small cavities of the membrane. Only the fluctuation modes with a wavelength larger than the particle diameter are relevant for the effective roughness of the membrane, while the small wavelength modes lead to an additional shift of the particle profile.

In Fig. 5, the same curves as in Fig. 4 are shown; every profile is now shifted by  $p_1$ . One can observe the changes of the tilting when  $\beta$  is increased. Clearly, this effect is a consequence of the effective roughness. Insets show the effective membrane-particle potential. From this, it is clear that as long as  $\beta$  becomes larger, the effective interaction tends to be more repulsive since the particles cannot access into the smaller cavities of the rough surface.

In Fig. 6 we show profiles for  $\beta = 1.0$  and different values of  $\alpha$ . With increasing  $\alpha$  the profiles become steeper. One can gain a better understanding on the role of  $\alpha$  by rescaling the  $z$ -axis with  $\xi_\perp^d$ . Interestingly, the inset shows that the profiles collapse onto a master curve. This means that the distribution of the molecules is governed by only one dimensionless parameter,  $\beta$ , by which the parameter space is reduced to one-dimension.

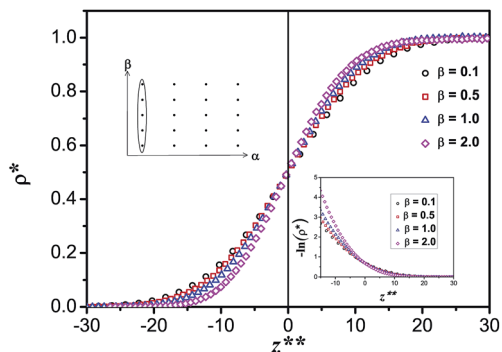


Fig. 5 Density profile from Fig. 4. A translational transformation is being applied by  $z^{**} = (z - z_0 - a_c - p_1)/a_c$  and the same rescaling for the density profiles as shown in Fig. 4 is assumed. As long as  $\beta$  increases a tilt on the profiles becomes more noticeable because particles cannot penetrate into those areas where the fast modes of the membrane take place.

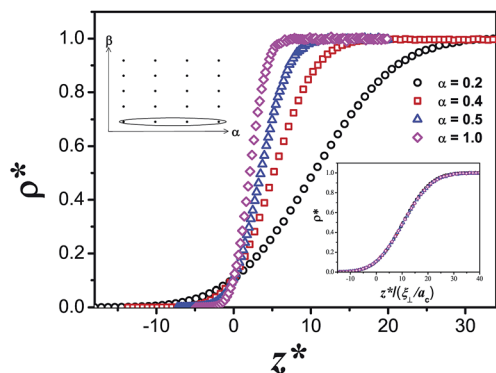


Fig. 6 Density profiles for different values of  $\alpha$  with  $\beta$  constant. The same rescaling as shown in Fig. 4 is assumed. The inset shows that by rescaling the  $z$ -axis defined as  $z^* = (z - z_0 - a_c)/a_c$  by  $z^*/(\xi_{\perp}^d/a_c)$  all profiles lie onto the same curve. On the top left, a schematic representation of the parameter space is drawn.

We performed further simulations for different values of  $\beta$  in order to explore the functional dependence of the shifting,  $p_1$  and tilting,  $p_2$ , as a function of  $\beta$ . In Fig. 7,  $p_1$  as a function of  $\beta$  is shown for two different values of  $\alpha = 0.2$  and  $0.4$ . The inset shows evidence that the shift depends only on the lateral correlation length of the membrane; the shifting is a monotonically increasing function of  $\beta$ . From the simulation point of view, it becomes more difficult to increase the value of  $\beta$  due to the required conditions for the simulation of the system, *i.e.*,  $d \gg \xi_{\perp}^d$ , with  $d$  being the separation between the membrane and a rigid wall, and  $\xi_{\parallel}^d/a \gg 1$ . Thus, simulations up to  $\beta = 4$  were performed in order to obtain results in a reasonably computing time. We should point out that larger values of  $\beta$  imply a higher number of particles in order to keep the same value of the bulk density.

In Fig. 8, the effective roughness,  $p_2$ , is shown for two different values of  $\alpha = 0.2$  and  $0.4$  as a function of  $\beta$ . The inset shows that when  $p_2$  is rescaled with  $\xi_{\perp}^d$ , it only depends on  $\beta$ . As long as  $\beta$  increases, the effective roughness becomes smaller compared with  $\xi_{\perp}^d$ . For  $\beta = 4.0$  this relative difference is about

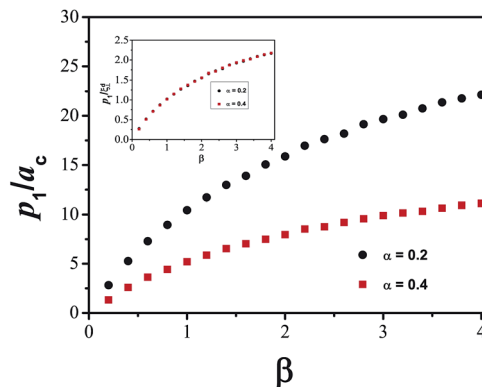


Fig. 7 Parameter  $p_1$ , as described in eqn (12), as a function of  $\beta$  for  $\alpha = 0.2$  and  $\alpha = 0.4$ . The inset shows that by rescaling with  $\xi_{\perp}^d$  the shift depends only on the lateral correlation of the membrane.

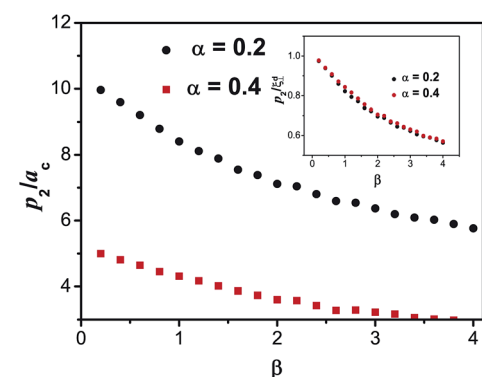


Fig. 8 Parameter  $p_2$ , as described in eqn (12), as a function of  $\beta$  for  $\alpha = 0.2$  and  $\alpha = 0.4$ . The inset shows the rescaled effective roughness.

40%, which is much larger than the change of the membrane roughness due to the presence of the particle that is roughly 3.2%, see Fig. 1.

Why does for low bulk densities the particle distribution at a fluctuating membrane only depend on one relevant parameter? The physical implications of our findings can be best explained by using a schematic representation. In Fig. 9, a particular configuration of the system is shown (on the left). The membrane is represented by the solid line; particles cannot penetrate into those regions below the dashed line, which can

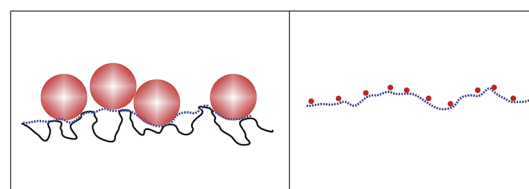


Fig. 9 Schematic representation of the membrane–biomolecule system. On the left, the solid line represents a particular configuration of the membrane. Particles with finite size cannot be located into the regions below the dashed line because there is no enough space. The dashed line represents an effective membrane which is less rough than the original one. On the right, the original system can be replaced by a less rough membrane in front of point-like particles.

be thought as an effective membrane. Therefore, the original system can be replaced by a less rough surface in front of point-like particles (on the right). This effective membrane has a roughness given by the parameter  $p_2$  which only depends on  $\beta$  as it is explicitly shown in Fig. 8.

## 4 Conclusions

In this work we have studied a fluctuating membrane in contact with spherical molecules. Particularly, we have focused our attention on the effect of the characteristic length scales of the system on the distribution of particles near to the membrane. We implemented Monte Carlo simulations to numerically evaluate the density profile in the vicinity of the membrane. We found that our simulation data agreed very well with analytical results in the limiting case of point-like particles in front of a fluctuating membrane.

To avoid particle–particle effects and to focus on the effects caused by the particle–membrane interaction, we considered the case of low densities. The parameter space was reduced to two dimensionless parameters: the ratio of the particle size with the two characteristic length scales of the membrane, namely, the lateral correlation length and the membrane roughness. After rescaling the length scales with the membrane roughness  $\xi_{\perp}^d$ , the particle density profiles depend only on  $\beta$ . If the lateral correlation of the membrane is smaller than the particle diameter ( $\beta$  is large), particles cannot penetrate into the resulting small cavities of the membrane, which increases the excluded volume of the particles. It follows that the membrane–particle systems can be replaced by a membrane with reduced roughness in front of point-like particles together with an additional shift of the profile due to the enhanced excluded volume. Hence, the density profile can be described by the same function as in the point-like case. Clearly, this behavior will not be valid anymore when the particle–particle interaction (high densities) has to be taken into account explicitly. The work along this line is currently under investigation.

## Acknowledgements

Financial support from PROMEP (Red Física de la Materia Blanda) and CONACyT (grant 102339/2008) is acknowledged. FCV and CF received support by BMBF Freiburg Initiative in Systems Biology 0313921 (FRISYS). R. C-P. also acknowledges the financial support provided by the Marcos Moshinsky fellowship 2013–2014.

## References

- 1 B. Alberts, D. Bray, J. Lewis, M. Raff, K. Roberts and J. D. Watson, *Molecular Biology of the Cell*, Garland Publishing, Inc. New York and London, New York, 3rd edn, 1994.
- 2 H. Lodish, D. Baltimore, A. Berk, S. L. Zipursky, P. Matsudaira and J. Darnell, *Molecular Cell Biology*, Macmillan, New York, 3rd edn, 1995.
- 3 S. O. Johanson, M. F. Crouch and I. A. Hendry, *Neurochem. Res.*, 1996, **21**, 779–785.
- 4 Z. Gou, H. Jiang, X. Xu, W. Duan and M. P. Mattson, *J. Biol. Chem.*, 2008, **283**, 1754–1763.
- 5 J. F. Nagle and S. Tristram-Nagle, *Biochim. Biophys. Acta, Rev. Biomembr.*, 2000, **1469**, 159–195.
- 6 D. Nelson, T. Piran and S. Weinber, *Statistical Mechanics of Membranes and Surfaces*, World Scientific, Singapore, 2004.
- 7 C. Fleck and R. R. Netz, *Phys. Rev. Lett.*, 2005, **95**, 128101.
- 8 C. Fleck and R. R. Netz, *Europhys. Lett.*, 2005, **70**, 341.
- 9 A. P. Minton and P. Allen, *Curr. Opin. Biotechnol.*, 1997, **8**, 65–69.
- 10 R. Castañeda-Priego, A. Rodríguez-López and J. M. Méndez-Alcaraz, *Phys. Rev. E: Stat., Nonlinear, Soft Matter Phys.*, 2006, **73**, 051404.
- 11 P. Bryk, R. Roth, K. R. Mecke and S. Dietrich, *Phys. Rev. E*, 2003, **68**, 031602.
- 12 R. Roth, B. Götzmann and S. Dietrich, *Phys. Rev. Lett.*, 1999, **83**, 448.
- 13 Z. W. Zhang and B. Neu, *Biophys. J.*, 2009, **97**, 1031–1037.
- 14 T. Bickel, *J. Chem. Phys.*, 2003, **118**, 8960–8968.
- 15 G. Brannigan, L. C. L. Lin and F. L. Brown, *Eur. Biophys. J.*, 2006, **35**, 104–124.
- 16 W. Helfrich, *Z. Naturforsch.*, 1973, **22**, 693.
- 17 R. Castañeda-Priego, F. Córdoba-Valdés and C. Fleck, *Rev. Mex. Fis.*, 2007, **53**, 475.
- 18 T. Bickel and C. M. Marques, *J. Nanosci. Nanotechnol.*, 2006, **6**, 2386–2395.
- 19 M. M. Müller, M. Deserno and J. Guven, *Phys. Rev. E: Stat., Nonlinear, Soft Matter Phys.*, 2005, **72**, 061407.
- 20 S. Semrau and T. Schmidt, *Soft Matter*, 2009, **5**, 3174–3186.
- 21 B. J. Reynwar and M. Deserno, *Soft Matter*, 2011, **7**, 8567–8575.
- 22 R. Lipowsky and E. Sackmann, *Structure and Dynamics of Membranes*, Elsevier, 1995.
- 23 U. Seifert, *Adv. Phys.*, 1997, **46**, 13–137.
- 24 J. O. Rädler, T. J. Feder, H. H. Strey and E. Sackmann, *Phys. Rev. E: Stat., Nonlinear, Soft Matter Phys.*, 1995, **51**, 4526.
- 25 A. Zilker, M. Ziegler and E. Sackmann, *Phys. Rev. A*, 1992, **46**, 7998.
- 26 W. Helfrich, *Z. Naturforsch.*, 1978, **33**, 305.
- 27 C. R. Safinya, E. B. Sirota, D. Roux and G. S. Smith, *Phys. Rev. Lett.*, 1989, **62**, 1134.
- 28 N. Gov and S. A. Safran, *Phys. Rev. E: Stat., Nonlinear, Soft Matter Phys.*, 2004, **69**, 011101.
- 29 N. Gov, A. G. Zilman and S. Safran, *Phys. Rev. Lett.*, 2003, **90**, 228101.
- 30 L. C. L. Lin and F. L. Brown, *Phys. Rev. E: Stat., Nonlinear, Soft Matter Phys.*, 2005, **72**, 011910.
- 31 H. Kaïdi, T. Bickel and M. Benhamou, *Europhys. Lett.*, 2005, **69**, 15.
- 32 Z. Yang, D. Zhang, Ateeq-ur-Rehman and L. Zhang, *Soft Matter*, 2012, **8**, 1901–1908.
- 33 C. Fleck, Fluctuating charged membranes, PhD Thesis, University of Konstanz, 2005.
- 34 T. Bickel, M. Benhamou and H. Kaïdi, *Phys. Rev. E: Stat., Nonlinear, Soft Matter Phys.*, 2004, **70**, 051404.
- 35 R. Lipowsky and H. G. Döbereiner, *Europhys. Lett.*, 1998, **43**, 219.